International Journal of Solid Materials
Vol. 1, Issue 2, 2019, Pages 155-169
Published Online on November 14, 2019

http://jyotiacademicpress.org

ELASTICITY SOLUTIONS TO THE STRESS INTENSITY FACTORS (SIFS) OF ORTHOTROPIC DOUBLE CANTILEVER BEAMS (DCBS) UNDER ANTIPLANE CRACKING

XIANG-FA WU

Department of Mechanical Engineering
North Dakota State University
Fargo, North Dakota 58108-6050
USA
e-mail: xiangfa.wu@ndsu.edu

Abstract

This paper reports the elasticity solutions to the stress intensity factors (SIFs) and strain energy release rates (ERRs) of orthotropic elastic double cantilever beams (DCBs) under antiplane cracking. The known solution of a single screw dislocation in an infinite anisotropic elastic medium and conformal mapping technique are employed for the solving procedure. The present solutions are able to examine the effect of specimen geometries on the SIF of the DCB specimens and overcome the geometrical limitation of the classic beam theory that all DCB fracture specimens rely on. The upper and lower limits of the SIFs are obtained in explicit expressions. In the limiting cases, the present solutions can recover the SIF solutions of conventional DCB specimens.

Keywords and phrases: double cantilever beam (DCB), stress intensity factor (SIF), energy release rate (ERR), composite materials.
Communicated by Kazem Reza Kashyzadeh.
Received July 16, 2019; Revised October 9, 2019

1. Introduction

Interlaminar fracture tests are commonly used for evaluating the delamination toughness of composite laminates. A number of fracture specimen configurations have been proposed in the last four decades, such as those based on double-cantilever beam (DCB) for pure Mode-I fracture tests, end-notched flexure (ENF), end-loaded split (ELS), and cracked lap shear (CLS) specimens for Mode-II fracture tests [1, 2], four-point end-notched flexure (4ENF), and mixed-mode bending specimens for mixed-mode tests [3, 4]. Accordingly, classic beam theory has been well formulated for extracting the stress intensity factors (SIFs) and strain energy release rates (ERRs) of these fracture specimens. To date, classic beam theory as a convenient engineering approach is broadly used for fracture study of isotropic elastic beams, and layered composite materials [5-7], and its validity is mainly examined by finite element analysis (FEA). Yet, classic beam theory is an engineering approach with obvious constraints of the specimen geometries in use, which may lead to noticeable deviation in the SIF estimate in the case of the crack length comparable to the beam height. This happens in the case of antiplane interlaminar fracture tests based on the DCB fracture specimens, where thick specimens are desirable in order to avoid torsional instability in the fracture test. Besides, antiplane (out-of-plane) delamination is one of the main concerns of material durability in laminated composites such as the common edge-delamination failure of fiber-reinforced polymer composites [8-11]. In an antiplane interlaminar fracture test, the beam thickness is typically selected large and the corresponding crack length is short by comparison with those employed in Mode-I and Mode-II fracture tests in order to avoid the possible torsional instability (twisting). As a result, the specimen geometries may break the assumptions of elementary beam theory. So far, little numerical simulation is available to confirm the validity of elementary beam theory for thick beams under antiplane loading. On the other hand, in the fracture study of cracked in-plane

elastic beams, no exact elasticity solutions are available for anisotropic DCB specimens, except for a few special in-plane cases of infinite-length isotropic, elastic strips with cracks embedded at the mid-plane [12-15]. However, in the case of antiplane deformation, exact elasticity solutions are usually available for cracked beams and joints due to the relatively simple mathematical formulation [16-19] by means of special mathematical techniques including dual integral equations, conformal mapping, etc. This provides an efficient way to finding the exact elasticity solution for antiplane composite DCB specimens.

In this work, we consider the exact SIFs and ERRs of an orthotropic DCB specimen under antiplane delaminating in order to provide the theoretical basis for data reduction of interlaminar fracture tests. The explicit solutions are obtained via solving the resulted antiplane elasticity problem with multiple boundary conditions (BCs) using the known solution of single screw dislocation in an infinite anisotropic, elastic medium, and conformal mapping technique [19-22]. Comparison of the present solutions with those based on elementary beam theory is made at varying aspect ratio of the specimen.

2. Problem Formulation and Solution Procedure

The composite DCB specimen under consideration in this study is modelled as an orthotropic solid, which is the continuum mechanics approach of a unidirectional fiber-reinforced polymer matrix composite (PMC). Firstly, the complex potential is introduced for such a cracked orthotropic medium under antiplane singularity (a single force or a screw dislocation). This complex potential will be further used to formulate the exact elasticity solution of the antiplane DCB specimen. Hereafter, the orthotropic medium is assumed with the $\xi\eta$-plane as a mirror plane. In this case, the in-plane and antiplane deformations are decoupled and can be treated independently. Under antiplane deformation, the out-of-plane (antiplane) displacement and stress components of an anisotropic body

(with the $\xi\eta$-plane as a mirror plane) may be expressed in terms of an analytic function $\varphi(\zeta)$ [22], i.e.,

$$\begin{aligned} u_3(\xi, \eta) &= -2\mathrm{lm}[B\varphi(\zeta)], \\ \sigma_{23}(\xi, \eta) &= -2\,\mathrm{Re}[\varphi'(\zeta)], \\ \sigma_{13}(\xi, \eta) &= 2\,\mathrm{Re}[\mu\varphi'(\zeta)], \end{aligned} \tag{1}$$

where the prime $(')$ denotes the derivative with respect to the complex variable $\zeta = \xi + \mu\eta$, and B and μ are two material constants defined as

$$\begin{aligned} B &= \sqrt{S_{44}S_{55} - S_{45}^2}, \\ \mu &= [S_{45} + i\sqrt{S_{44}S_{55} - S_{45}^2}\,]/\,S_{55}, \end{aligned} \tag{2}$$

S_{ij} are the elements of the material compliance matrix. In the case of orthotropic material, $B = \sqrt{S_{44}S_{55}}$ and $\mu = i\sqrt{S_{44}\,/\,S_{55}}$ is a positive imaginary.

Introduce an arbitrary antiplane singularity being located at (ξ_0, η_0) in an infinite orthotropic medium embedded with a semi-finite crack along the negative η-axis as shown in Figure 1. The complex displacement potential $\varphi(\zeta)$ for this problem has been given in the literature [22]:

$$\varphi'(\zeta) = \frac{q}{\zeta - \zeta_0} + \frac{q}{\zeta - \zeta_0}\left[\left(\frac{\zeta_0}{\zeta}\right)^{1/2} - 1\right] + \frac{\overline{q}}{\zeta - \overline{\zeta}_0}\left[\left(\frac{\overline{\zeta}_0}{\zeta}\right)^{1/2} - 1\right]. \tag{3}$$

In the above, the prime denotes the derivative with respect to the complex variable ζ, $\zeta_0 = \xi_0 + \mu\eta_0$, and q is the quantity of the antiplane singularity defined as:

$$q = -\frac{b}{4\pi B} + \frac{ip}{4\pi}, \tag{4}$$

where b is the Burgers vector of the screw dislocation and p is the line-force. The SIF and ERR induced by this antiplane singularity can be evaluated as [22]:

$$K_{III} = \lim_{\xi \to 0} -2\sqrt{2\pi\xi}\phi'(\xi), \quad G_{III} = \frac{B}{2} K_{III}^2. \tag{5}$$

In the particular case of an antiplane singularity in an infinite orthotropic medium embedded with a semi-infinite crack, the corresponding SIF is:

$$K_{III} = \sqrt{2\pi}\left[\frac{q}{(\zeta_0)^{1/2}} + \frac{\overline{q}}{(\overline{\zeta_0})^{1/2}} \right]. \tag{6}$$

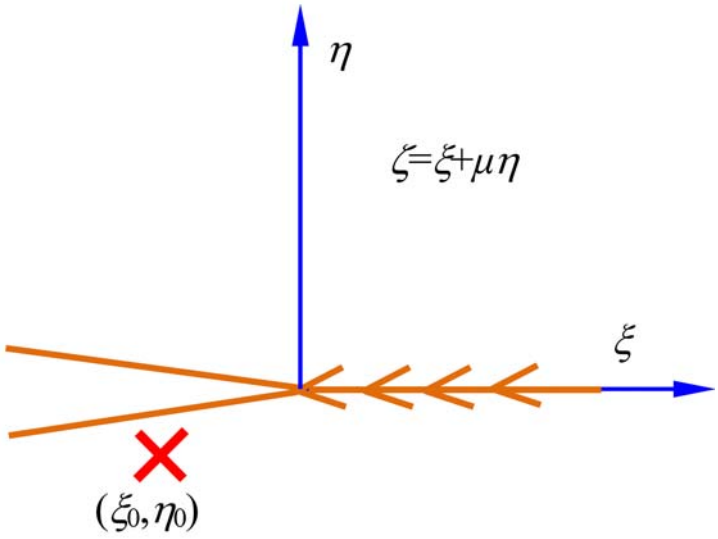

Figure 1. An orthotropic elastic medium (ζ-plane) under antiplane singularity.

In the above, the displacement potential $\varphi(\zeta)$ is an analytic function with respect to ζ. Therefore, the displacement solution of an orthotropic DCB specimen, as illustrated in Figure 2, can be constructed by using relations (3) and (4) and the conformal mapping technique. Consider the

orthotropic DCB specimen with the crack embedded at the mid-plane and subjected to an antiplane singularity at one arm at $(x_0,\ y_0),$ as shown in Figure 3(a), where a and H denote the crack length and the beam half-width, respectively. Introduce the conformal mapping:

$$\varsigma = \frac{g^2(z+a)}{g^2(a)} - 1, \tag{7}$$

with

$$g(z) = \sinh\left(\frac{\pi z}{2|\mu|H}\right), \tag{8}$$

which maps the region of the orthotropic DCB onto the entire plane with a semi-infinite cut along the negative ξ-axis, as shown in Figure 3(b). Herein, the complex variable z is defined as $z = x + \mu y,$ and $|\bullet|$ denotes the absolute value of a complex variable. Substitution of (7) and (8) into (6) leads to the SIF of the orthotropic DCB under an antiplane singularity at z_0

$$K_{III} = \frac{2\sqrt{2\pi}}{\sqrt{\pi a}}\sqrt{\frac{\pi a}{|\mu|H}\sinh\left(\frac{\pi a}{|\mu|H}\right)} \Big/ \mathrm{Re}\left\{-iq\sqrt{\cosh\left(\frac{\pi a}{|\mu|H}\right) - \cosh\left[\frac{\pi(z_0+a)}{|\mu|H}\right]}\right\}. \tag{9}$$

Here, Re( ) is the real part of an analytic function, and $z_0 = x_0 + \mu y_0.$ The corresponding ERR can be obtained by inserting (9) into (6). Relation (9) can be used as the Green's function to construct the SIFs and ERRs for a large family of antiplane DCB specimens subjected to arbitrary antiplane loadings. In particular, this solution can be used for examining the effect of geometries in the SIFs as a correction of the elementary beam theory used for antiplane DCB samples. Furthermore, in the limiting case of isotropic materials, i.e., $|\mu| = 1,$ relation (9) can recover these given in the literature [20, 23].

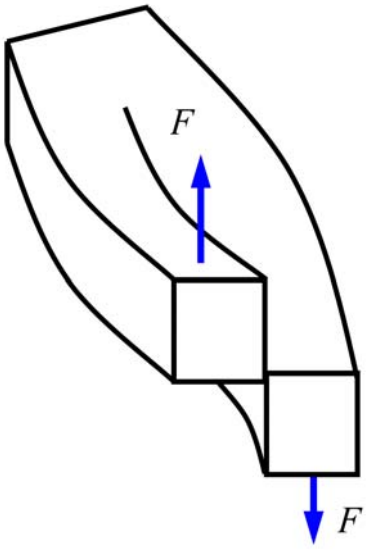

Figure 2. Schematic of a DCB specimen in antiplane fracture test.

3. Examples and Discussions

3.1. Orthotropic DCB specimens with concentrated loads acting within the beam arms and crack surfaces

First, consider an orthotropic DCB beam with the coordinate system as shown in Figure 4. The beam is loaded with a pair of concentrated antiplane forces (in opposite directions) of magnitude P at two symmetric points (x_0, y_0) and $(x_0, -y_0)$ to simulate a DCB antiplane fracture test as shown in Figure 4(a). By setting $q = iP/(4\pi)$ and $z_0 = z_0 \pm \mu y_0$ in (9) and revoking the method of superposition, it leads to the SIF:

$$K_{III} = \frac{\sqrt{2}P}{\sqrt{\pi a}}\sqrt{\frac{\pi a}{|\mu|H}\sinh\left(\frac{\pi a}{|\mu|H}\right)} \Big/ \mathrm{Re}\left\{\sqrt{\cosh\left(\frac{\pi a}{|\mu|H}\right) - \cosh\left[\frac{\pi(x_0 + a + \mu y_0)}{|\mu|H}\right]}\right\}. \tag{10}$$

In the above, once the location of the force is given, the SIF can be determined in closed-form. This solution can be used for examining the effects of the force location, specimen geometries, and crack length on the SIF value.

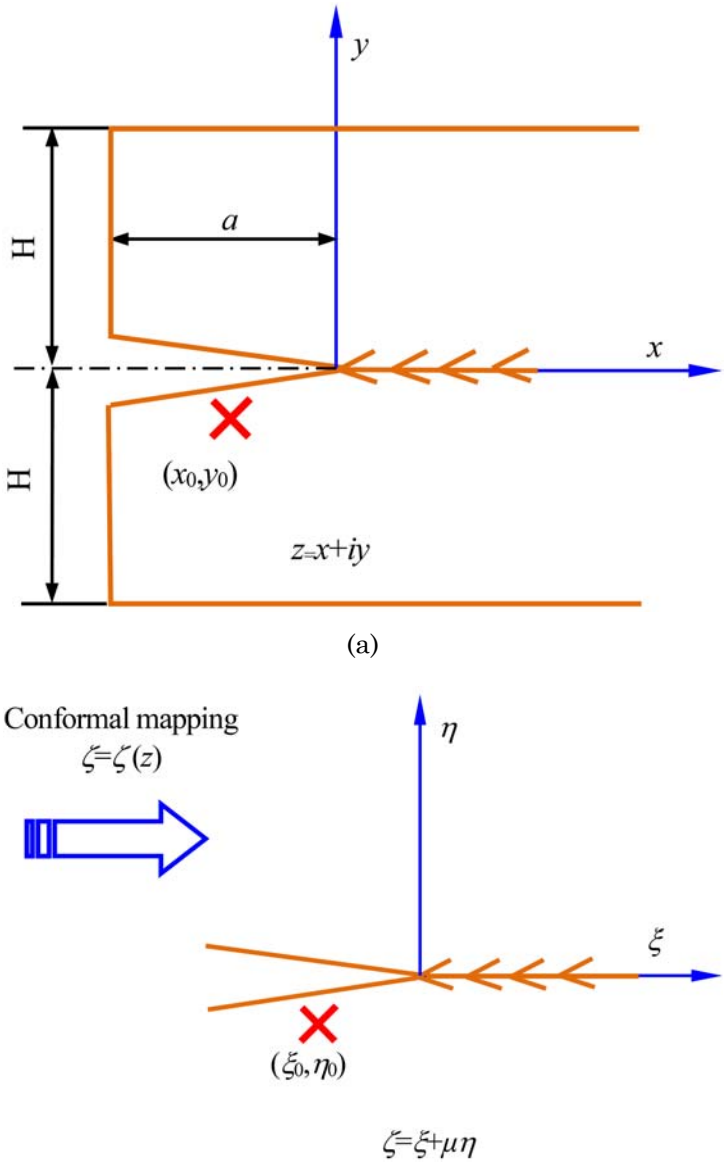

Figure 3. A cracked orthotropic DCB specimen under an antiplane singularity: (a) an edge-cracked orthotropic elastic layer (z-plane); (b) a semi-infinite crack in elastic medium (ζ-plane).

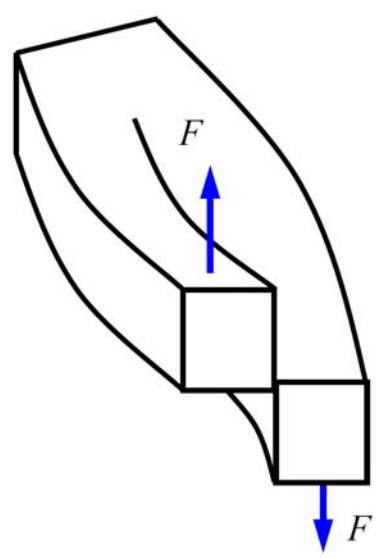

(a)

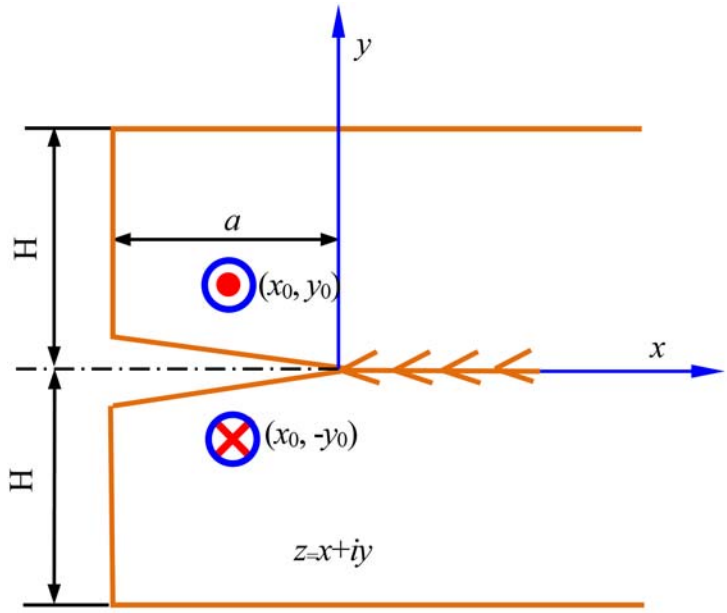

(b)

Figure 4. A cracked orthotropic DCB specimen under action of a pair of concentrated forces in opposite directions: (a) physical model; (b) geometrical configuration of specimen (z-plane).

In the limiting case of the pair of concentrated forces located at crack surfaces, i.e., $y_0 = 0$, relation (10) reduces to the upper limit of the SIF for given force magnitude P and location x_0:

$$K_{III}^{\text{upper}} = \frac{\sqrt{2}P}{\sqrt{\pi a}}\sqrt{\frac{\pi a}{|\mu|H}\sinh\left(\frac{\pi a}{|\mu|H}\right)} \Big/ \sqrt{\cosh\left(\frac{\pi a}{|\mu|H}\right) - \cosh\left[\frac{\pi(x_0 + a)}{|\mu|H}\right]}, \tag{11}$$

where $x_0 < 0$ for a physically meaningful fracture specimen, i.e., forces acting behind the crack tip. When $x_0 > 0$, no SIF exists according to (10). Furthermore, when the pair of concentrated forces are located at the beam surfaces, i.e., $y_0 = H$, relation (10) leads to the lower limit of the SIF for given force magnitude P and location x_0:

$$K_{III}^{\text{lower}} = \frac{\sqrt{2}P}{\sqrt{\pi a}}\sqrt{\frac{\pi a}{|\mu|H}\sinh\left(\frac{\pi a}{|\mu|H}\right)} \Big/ \sqrt{\cosh\left(\frac{\pi a}{|\mu|H}\right) + \cosh\left[\frac{\pi(x_0 + a)}{|\mu|H}\right]}. \tag{12}$$

Therefore, relations (11) and (12) present the exact upper and lower limits of the SIF for a pair of concentrated forces applied symmetrically on an orthotropic DCB specimen. The ratio of the upper SIF limit over the lower SIF limit is:

$$\rho = \frac{K_{III}^{\text{upper}}}{K_{III}^{\text{lower}}} = \sqrt{\cot\left(\frac{-\pi x_0}{2|\mu|H}\right)\frac{1 + \tanh\left(\frac{\pi x_0}{2|\mu|H}\right)\tanh\left(\frac{\pi a}{|\mu|H}\right)}{\tanh\left(\frac{\pi x_0}{2|\mu|H}\right) + \tanh\left(\frac{\pi a}{|\mu|H}\right)}}. \tag{13}$$

As a limiting case of geometry, by letting $a \to \infty$, the SIF solution (10) can be reduced for that of a semi-infinite antiplane crack embedded at the mid-plane of an infinite orthotropic layer loaded with the pair of antiplane forces:

$$K_{III} = P\sqrt{\frac{2}{|\mu|H}} \Big/ \operatorname{Re}\left\{\sqrt{1 - \exp\left(\frac{\pi x_0}{|\mu|H}\right)\left[\cos\left(\frac{\pi y_0}{H}\right) + i\sin\left(\frac{\pi y_0}{H}\right)\right]}\right\}. \tag{14}$$

Similarly, by setting $y_0 \to 0$, relation (14) leads to the SIF of the infinite layer with the pair of loads acting on the crack surfaces:

$$K_{III}^{\text{upper}} = P\sqrt{\frac{2}{|\mu|H}} \Big/ \sqrt{1 - \exp(\frac{\pi x_0}{|\mu|H})}. \tag{15}$$

Besides, when $y_0 \to H$, relation (14) yields the SIF of the infinite layer with the pair of loads acting on the beam surfaces:

$$K_{III}^{\text{lower}} = P\sqrt{\frac{2}{|\mu|H}} \Big/ \sqrt{1 + \exp(\frac{\pi x_0}{|\mu|H})}. \tag{16}$$

In this limiting case, the corresponding ratio of the upper SIF limit over the lower one is:

$$\rho = \frac{K_{III}^{\text{upper}}}{K_{III}^{\text{lower}}} = \sqrt{\cot(\frac{-\pi x_0}{2|\mu|H})}. \tag{17}$$

Relation (17) can also be obtained by letting $a / H \to \infty$ in relation (13).

To determine the SIF of uniformly distributed forces of density p acting on the entire crack surfaces, the SIF value can be determined by integrating (10) with respect to x_0 in the interval of $[-a, 0]$:

$$K_{III} = p\sqrt{\pi a}\,\frac{2}{\pi}\sqrt{\frac{2|\mu|H}{\pi a}\tanh(\frac{\pi a}{2|\mu|H})}K[(\frac{\pi a}{2|\mu|H})], \tag{18}$$

where $K(\ )$ is the complete elliptic integral of the first kind. In the limiting case of isotropic materials, i.e., $|u| \to 1$, result (18) recovers those given by Li [18] using the technique of dual integral equations and Wu and Dzenis [20] using conformal mapping technique.

3.2. Orthotropic DCB specimens with loads acting at specimen heads

In this case, by setting $x_0 = -a$ in relation (10), the SIF corresponds to the antiplane orthotropic DCB specimens with the pair of antiplane forces acting at the specimen ends symmetrically as:

$$K_{III} = \frac{\sqrt{2}P}{\sqrt{\pi a}} \sqrt{\frac{\pi a}{|\mu|H} \sinh\left(\frac{\pi a}{|\mu|H}\right)} \Big/ \sqrt{\cosh\left(\frac{\pi a}{|\mu|H}\right) - \cos\left(\frac{\pi y_0}{H}\right)}. \tag{19}$$

Similarly, when the specimen loaded with uniformly distributed force of density p, the corresponding SIF can be determined by integrating (19) with respect to y_0 in the interval of $[0, H]$:

$$K_{III} = p\sqrt{\pi a}\,\frac{2}{\pi} \sqrt{\frac{H}{\pi|\mu|a} \sinh\left(\frac{\pi a}{|\mu|H}\right)} \int_0^{\pi/2} \left[\sinh^2\left(\frac{\pi a}{2|\mu|H} + \sin^2\varphi\right)\right]^{-1/2} d\varphi. \tag{20}$$

The ERRs of the above cracks can be determined by using the relationship between the ERR and SIF as given in (5).

4. Concluding Remarks

The displacement potential, SIF and ERR of orthotropic DCB specimens subjected to antiplane crack were determined in closed-form by simultaneously using the known solution of single screw dislocation in anisotropic medium and conformal mapping technique. The given explicit solutions can be directly used for experimental data reduction. Specifically, the given results (10), (11), and (12) can be utilized to examine the effect of specimen geometry on the SIF and ERR of a given DCB specimen. Furthermore, these elasticity SIF solutions overcome the constraints of the elementary beam theory, and therefore can be used as the corrections of the SIF solutions based on beam theory. Moreover,

since the present solutions are determined in the view of dislocation theory, the general solutions (9) and (10) can be considered as Green's functions to construct a large family of solutions in orthotropic DCB specimens related to realistic fracture phenomena such as crack kink, curved cracks, etc. These solutions are generally difficult to be solved directly using method of dual integral equations.

References

[1] L. A. Carlsson and P. B. Pipes, Experimental Characterization of Advanced Composite Materials, New Jersey: Prentice-Hall, 1987.

[2] T. E. Tay, Characterization and analysis of delamination fracture in composites: An overview of developments from 1990 to 2001, Applied Mechanics Review 56(1) (2003), 1-32.

DOI: https://doi.org/10.1115/1.1504848

[3] C. Schuecker and B. D. Davidson, Evaluation of the accuracy of the four-point bend end-notched flexure test for mode II delamination toughness determination, Composites Science and Technology 60(11) (2000), 2137-2146.

DOI: https://doi.org/10.1016/S0266-3538(00)00113-5

[4] R. H. Martin, Interlaminar fracture characterization, Key Engineering Materials 120-121 (1996), 329-346.

DOI: https://doi.org/10.4028/www.scientific.net/KEM.120-121.329

[5] Z. G. Suo and J. W. Hutchinson, Interface crack between two elastic layers, International Journal of Fracture 43(1) (1990), 1-18.

DOI: https://doi.org/10.1007/BF00018123

[6] J. W. Hutchinson and Z. Suo, Mixed mode cracking in layered materials, Advances in Applied Mechanics 29 (1991), 63-191.

DOI: https://doi.org/10.1016/S0065-2156(08)70164-9

[7] W. C. Liao and C. T. Sun, The determination of mode III fracture toughness in thick composite laminates, Composites Science and Technology 56(4) (1996), 489-499.

DOI: https://doi.org/10.1016/0266-3538(96)00009-7

[8] R. B. Pipes and N. J. Pagano, Interlaminar stresses in composite laminates under uniform axial extension, Journal of Composite Materials 4(4) (1970), 538-548.

DOI: https://doi.org/10.1177/002199837000400409

[9] X. F. Wu and Y. A. Dzenis, Experimental determination of probabilistic edge-delamination strength of a graphite-fiber/epoxy composite, Composite Structures 70(1) (2005), 100-108.

DOI: https://doi.org/10.1016/j.compstruct.2004.08.016

[10] X. F. Wu and A. L. Yarin, Recent progress in interfacial toughening and damage self-healing of polymer composites based electrospun and solution-blown nanofibers: An overview, Journal of Applied Polymer Science 130(4) (2013), 2225-2237.

DOI: https://doi.org/10.1002/app.39282

[11] D. Geng, Y. Liu, Z. Shao, Z. Lu, J. Cai, X. Li, X. Jiang and D. Zhang, Delamination formation, evaluation and suppression during drilling of composite laminates: A review, Composite Structures 216 (2019), 168-186.

DOI: https://doi.org/10.1016/j.compstruct.2019.02.099

[12] T. Y. Fan, Exact-solutions of semi-infinite crack in a strip, Chinese Physics Letter 7(9) (1990), 402-405.

DOI: https://doi.org/10.1088/0256-307X/7/9/006

[13] D. W. Shen and T. Y. Fan, Exact solution of two semi-infinite collinear cracks in a strip, Engineering Fracture Mechanics 70(6) (2003), 813-822.

DOI: https://doi.org/10.1016/S0013-7944(02)00083-8

[14] X. F. Wu, E. Lilla and W. S. Zou, A semi-infinite interfacial crack between two bonded dissimilar elastic strips, Archive of Applied Mechanics 72(8) (2002), 630-636.

DOI: https://doi.org/10.1007/s00419-002-0240-y

[15] X. F. Wu, Y. A. Dzenis and T. Y. Fan, Two semi-infinite interfacial cracks between two bonded dissimilar elastic strips, International Journal of Engineering Science 41(15) (2003), 1699-1710.

DOI: https://doi.org/10.1016/S0020-7225(03)00107-1

[16] G. C. Sih, Handbook of Stress-Intensity Factors, Bethlehem, Pennsylvania: Lehigh University, 1973.

[17] H. Tada, P. C. Paris and C. G. Irwin, The Stress Analysis of Cracks, Hellertown, Pennsylvania: Del Research Corporation, 1973.

[18] X. F. Li, Closed-form solution for a mode-III interface crack between two bonded dissimilar elastic layers, International Journal of Fracture 109(2) (2001), 3-8.

DOI: https://doi.org/10.1023/A:1010960305812

[19] X. F. Wu, Y. A. Dzenis and E. Gokdag, Edge-cracked orthotropic bimaterial butt joint under antiplane singularity, International Journal of Nonlinear Sciences and Numerical Simulations 5(4) (2004), 347-354.

DOI: https://doi.org/10.1515/IJNSNS.2004.5.4.347

[20] X. F. Wu and Y. A. Dzenis, Closed-form solution for a mode-III interfacial edge crack between two bonded dissimilar elastic strips, Mechanics Research Communications 29(5) (2002), 407-412.

DOI: https://doi.org/10.1016/S0093-6413(02)00317-8

[21] X. F. Wu, Y. A. Dzenis and W. S. Zou, Interfacial edge crack between two bonded dissimilar orthotropic strips under antiplane point loading, Zeischrift für Angewandte Mathematik und Mechanik 83(6) (2003), 419-422.

DOI: https://doi.org/10.1002/zamm.200310063

[22] Z. Suo, Singularities, interfaces and cracks in dissimilar anisotropic media, Proceedings of the Royal Society A: Mathematical, Physical and Engineering Sciences 427(1873) (1990), 331-358.

DOI: https://doi.org/10.1098/rspa.1990.0016

[23] V. Petrova, S. Schmauder, M. Ordyan and A. Shashkin, Revisit of antiplane shear problems for an interface crack: Does the stress intensity factor for the interface model III crack depend on the bimaterial modulus?, Engineering Fracture Mechanics 216 (2019); Article 106524.

DOI: https://doi.org/10.1016/j.engfracmech.2019.106524

■